Atomic structure of high-index Ge surfaces consisting of periodic nanoscale facets

Zheng Gai, R. G. Zhao, Hang Ji, Xiaowei Li, and W. S. Yang*
Mesoscopic Physics Laboratory and Department of Physics, Peking University, Beijing 100871, China
(Received 14 May 1997)

We have studied the clean and well-annealed Ge(103) surface with scanning tunnel microscopy (STM) and low-energy electron diffraction, whose morphology exhibits large 1×4 reconstructed (103) terraces along with tentlike protrusions consisting of (105), {216}, and {8 1 16} facets. On the basis of the STM images, atomistic models have been proposed for the $(103)1\times4$, the $(216)1\times1$, and the $(105)1\times2$ surfaces for further investigations. The former two surfaces consist of only nanoscale (113) terraces and hence belong to the (113) family while the latter consists of only nanoscale (001) terraces and thus belongs to the (001) family. The mini (001) terraces that the $(105)1\times2$ reconstruction consists of, form a checkerboard pattern, thus implying a stress-relaxation driving force behind the reconstruction. These surface structures demonstrate that Herring's faceting theorem could be valid down to atomic scales, provided that the atomic-scaled facets could be connected into a large surface by low-energy edges and/or corners. [S0163-1829(97)01943-7]

INTRODUCTION

As a result of the intensive investigation of semiconductor surfaces carried out in the past decades, not only has atomic structure of the most important low-index Si surfaces, i.e., Si(111) and Si(001), been known[1,2] but also morphology of these surfaces and their vicinal surfaces as well as the driving forces behind them.[3–22] On the basis of that, recently, the atomic structure of the most stable high-index surface Si(113) has been studied and disclosed.[23–27] More recently, atomic structure and morphology of some other Si(hhk) surfaces have also been revealed,[28–31] and the results indicate that investigation of high-index Si surfaces is still necessary and not easy even with Herring's theorem on surface faceting[32] and the equilibrium shape of Si (Refs. 33 and 34) in mind. One can easily find that, apart from the only low-index surface that has received less attention, i.e., Si(101),[35] high-index surfaces belonging to the Si($h0k$) series and the Si(hkh) series have been neglected almost completely.

On the other hand, Ge surfaces have been receiving much less attention than their silicon counterpart,[1] only because of their less importance in applications. From the basic scientific point of view, however, investigation of germanium surfaces should not be neglected, since if we could compare germanium surfaces with their silicon counterpart our knowledge would certainly become more systematic. According to this consideration, we have been carrying out a series of investigations on the clean Ge surfaces of (001),[36,37] (111),[38,39] and (113),[40,41] as well as (112), (114), and (115),[42] along with many metal/Ge interfaces.[43–51]

In the course of our recent Ga/Ge(103) work, we noticed that the clean Ge(103) surface is not only very stable against cycles of ion bombardment and annealing but is also able to give rise to very nice $(103)1\times4$ patterns.[51] In view of this fact, and that the (103) surface of neither Si nor Ge has been known, in the present paper, by means of scanning tunneling microscopy (STM) and low-energy electron diffraction (LEED), we have studied the atomic structure of the Ge(103) surface reconstruction and that of the (216) and (105) facets, which can often be seen on the Ge(103) surface and are also very stable. Models of the Ge(103)1×4, Ge(216)1×1, and Ge(105)1×2 reconstructions have been proposed for further investigations.

EXPERIMENT

The experiment was carried out in the UHV system that has been used in recent studies.[39,40,46,47] Briefly, the system consists of a main chamber, where LEED, Auger electron spectroscopy (AES), and a homemade scanning tunneling microscope are installed, and a sample preparation chamber, where ion bombardment and annealing are carried out. In STM experiments the bias voltage is applied to the sample and the tip is grounded. The constant-current mode of the STM was used throughout the work and the scanning rate was from 200 to 2000 Å/sec. All images shown here were acquired with the ac mode, i.e., differential or local-contrast-enhanced mode, unless otherwise mentioned. The tip was made out of W wire with electrochemical etching. The Ge(103) sample, which had a size of $7\times7\times0.5\ \mathrm{mm}^3$ and a precision of $\pm0.5°$, was cut from a single-crystal rod with a resistivity of 40–50 Ω cm. After several cycles of ''argon-ion bombardment plus subsequent annealing'' a clean and well-ordered surface can always be obtained, as verified by AES and LEED.

OBSERVATIONS

Looking at the clean and well-annealed Ge(103) surface with LEED, we noticed that when the incidence-beam energy is increased most diffraction spots move towards a common center where the (00) spot of the (103) surface exists while some others move towards another (00) spot. This indicates the existence of some facets on the (103) surface. According to the relative position of the two (00) spots, we know that the facets were (105). Moreover, LEED also tells that the (103) surface was 1×4 reconstructed while the (105) facets were 1×2 reconstructed. A typical LEED pattern obtained from the surface is shown in Fig. 1 along with a schematic drawing showing which spots belong to which.

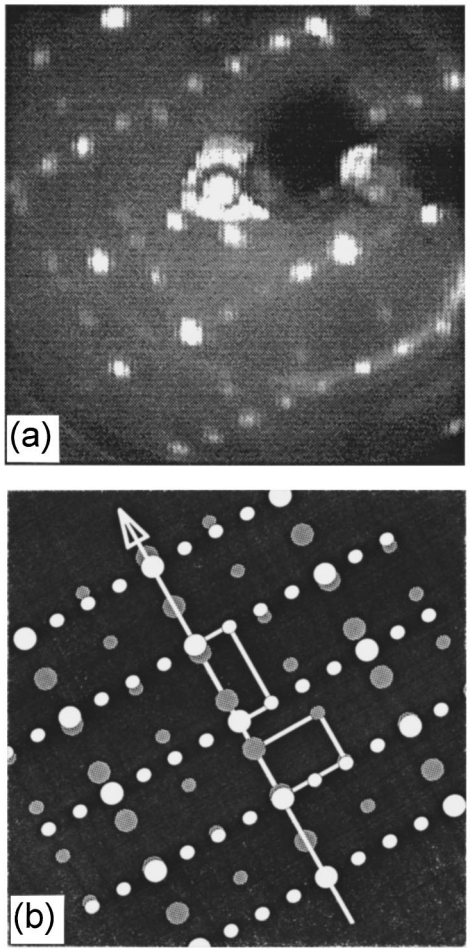

FIG. 1. (a) LEED pattern (27 eV) obtained from the clean and well-annealed Ge(103)1×4 surface, but with some diffraction spots from the (105)1×2 facets also visible. (b) A schematic drawing of the pattern in (a), showing which spots belong to which surface reconstruction. The white and gray circles represent the spots of the (103)1×4 and (105)1×2 reconstructions, respectively, while the large and small circles represent the integral- and fractional-order spots, respectively. The arrow points to the [301] direction. A unit cell of both reconstructions is also shown. Not shown is the round shadow of the sample holder at the center of (a).

Large-scale STM images of the same clean and well-annealed surface show that it consists of (103) terraces and many large or small tentlike protrusions with a similar shape (Fig. 2). Shown in Fig. 3(a) is the image of such a protrusion. Combining the LEED result just mentioned above with this image, we can easily determine which facet of the protrusion is (105). Then we can determine the index of the other facets, i.e., {216} and {8 1 16} [see Fig. 3(b)] according to the intersecting lines they form with the (103) surface and the (105) facet and with each other, although we have less confidence on the index of the {8 1 16} facets because the intersecting lines they form with the (103) and other facets are not very well defined. We believe that these tentlike protrusions would not appear if the original surface were a perfect (103) surface without any local ups and downs. It is interesting to point out that before looking at the surface with the scanning tunneling microscope we had not seen any spots other than those from the (103)1×4 surface and (105)1×2 facets

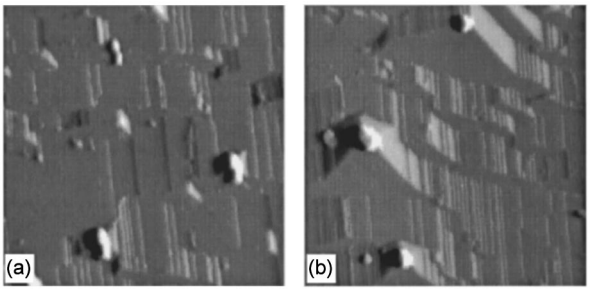

FIG. 2. Large-scale STM images of the clean and well-annealed Ge(103) surface, showing the morphology of the surface: many large and small tentlike protrusions coexist with large (103) terraces and small but long (216) and ($2\bar{1}6$) facets. (a) 2050×2050 Å^2, 5.0 V, 0.5 nA. (b) 2144×2144 Å^2, 5.0 V, 0.5 nA.

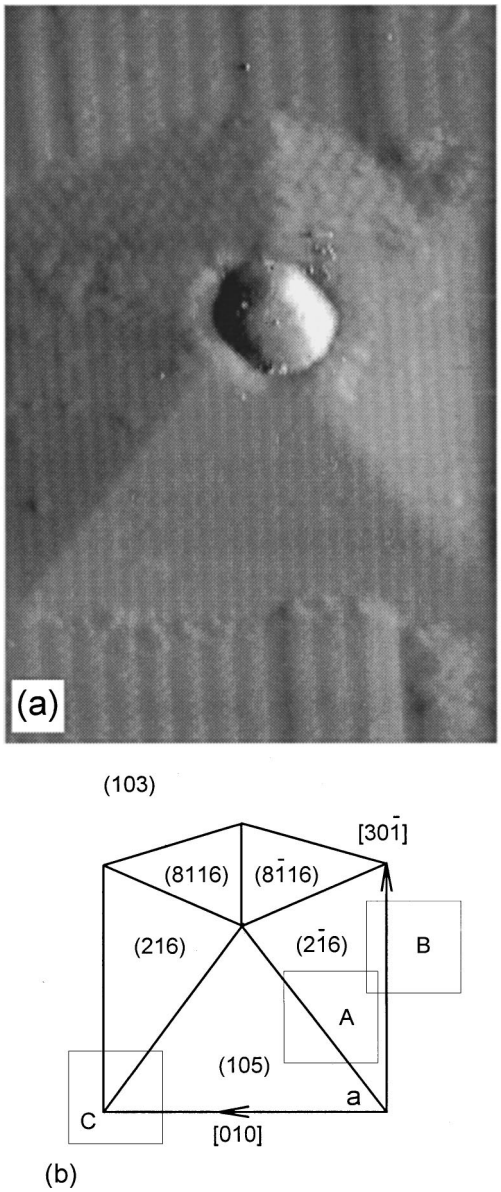

FIG. 3. (a) STM image (343 Å$\times$520 Å, 1.5 V, 0.5 nA) of a tentlike protrusion imaged in Fig. 2(b). (b) A schematic drawing of (a), showing the index of the facets of the protrusion.

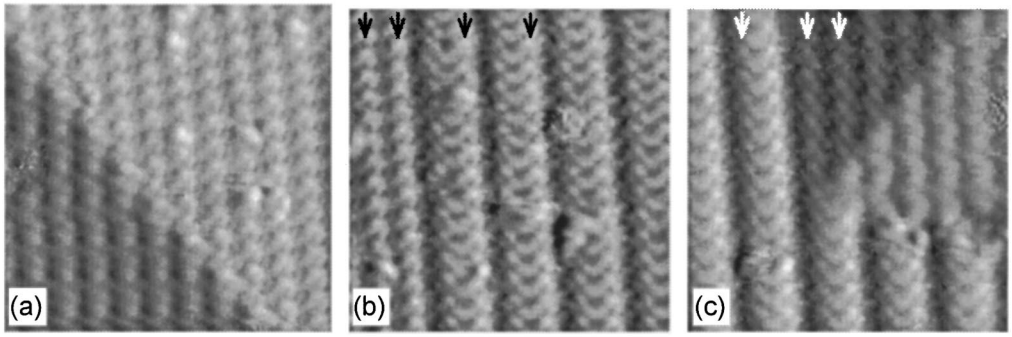

FIG. 4. Enlarged STM images of the square areas outlined in Fig. 3(b). (a) From area *A*, $119\times119\ \text{Å}^2$, 1.5 V, 0.5 nA. (b) From area *B*, $110\times110\ \text{Å}^2$, 1.5 V, 0.5 nA. (c) From area *C*, $112\times112\ \text{Å}^2$, 1.5 V, 0.5 nA.

while after we saw the {216} facets with the scanning tunneling microscope we looked at the surface with LEED again but we still could not find any {216} spots. The reason might be that, apart from the triangular {216} facets that belong to the tentlike protrusions, there are many stripped {216} facets (see Fig. 2), and it is these narrow {216} strips that make the {216} LEED spots elongated in the direction perpendicular to [301] so that they overlap with each other becoming the background, exactly on which the $(103)1\times4$ spots are superimposed.

It is worthwhile to point out that all the tentlike protrusions appearing on the (103) surface are of the same kind, none of them consisting of (104) or (102) facets, although protrusions with such facets ought to be kinetically easier to form and the (102) surface was reported to be stable.[52] This fact indicates that the (104) and (102) surfaces, different from the (105), (216), and (8 1 16) surfaces, are unstable against formation of facets.

To know more about the (103) surface and the facets, we need to consider more details in their STM images. Three high-resolution images are thus shown in Fig. 4, which are enlarged images obtained from the protrusion imaged in Fig. 3(a): Figs. 4(a), 4(b), and 4(c) were obtained from the square area *A*, *B*, and *C* outlined in Fig. 3(b), respectively. Comparing the upper-right portion of Fig. 4(a) or the left strip of Fig. 4(b), where the (216) facet is imaged, with the major part of Fig. 4(b), where the $(103)1\times4$ surface is imaged, one can find that both structures consist of strips lying along the [301] direction, that the width of a (103) strip is twice as large as that of a (216) strip, and that the structure of a (216) strip is the same as that of the right-hand side of a (103) strip. Similarly, by comparing the lower-left portion with the central-upper triangular portion of Fig. 4(c) one can find that the structure of a (216) strip is the same as that of the left-hand side of a (103) strip. In other words, each $(103)1\times4$ strip consists of a (216) strip and a (216) strip. Because the (216) and (216) surfaces form an angle of 18° this means that the $(103)1\times4$ surface must look like many parallel ridges and valleys lying along the [301] direction. This can be clearly seen from dc-mode images of the surface [see Fig. 5(a)].

MODELS AND DISCUSSIONS

Now, we try to find the atomic structure of the $(103)1\times4$ surface from its STM images. However, it has been known since the very beginning of STM that care has to be taken if one wants to correlate STM features with the atomic structure of semiconductor surfaces since it is the local density of states, instead of the surface topology, that directly determine the STM features.[53] In order to be able to extract surface topological information out of STM images while, on the other hand, not to be involved in tedious image calculations, it has been suggested to use the *atomic image*, which is defined as the *average of a pair of filled- and empty-state images collected simultaneously* from a surface, as an *approximation* of the surface-atomic structure.[40] This has been successfully used in recent works to deduce the atomic structure of surfaces from their STM images.[40,50,54] Accordingly, in Figs. 5(b) and 5(c) is a pair of STM images of the $Ge(103)1\times4$ surface, while the atomic image obtained from them is given in Fig. 5(d).

To correlate the features in this atomic image with the atomic structure of the $Ge(103)1\times4$ surface, we look first at the truncated (103) surface schematically shown in Fig. 6(a): the surface has no symmetry but a glide line; there are four surface atoms carrying one or two dangling bonds in each

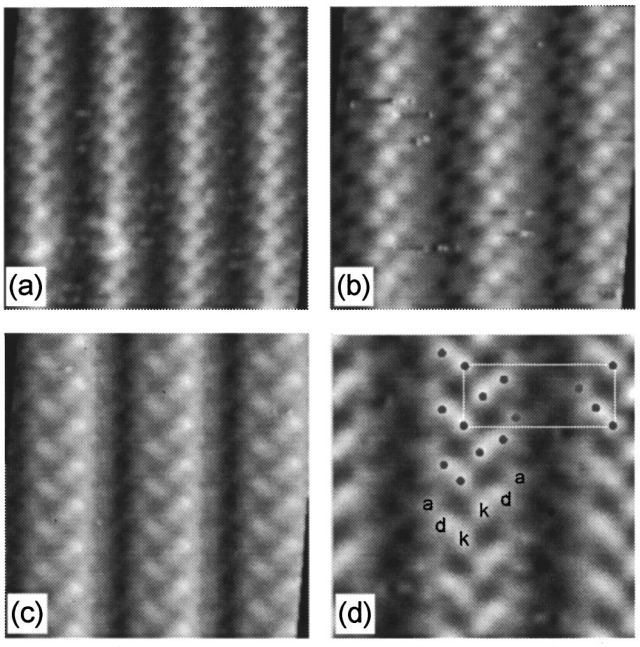

FIG. 5. STM images of the $Ge(103)1\times4$ surface. (a) dc mode, $89\times89\ \text{Å}^2$, -1.5 V, 1.0 nA. Note that the top of the ridges and the bottom of the valleys are glide line. (b) $64\times64\ \text{Å}^2$, -1.5 V, 1.0 nA. (c) $64\times64\ \text{Å}^2$, 1.5 V, 1.0 nA, acquired simultaneously with (b). Note that the glide-line symmetry is obscured a bit due to the using of the ac mode. (d) Atomic image (see text) obtained from (b) and (c). $46\times46\ \text{Å}^2$. Note that the glide-line symmetry is repaired through processing.

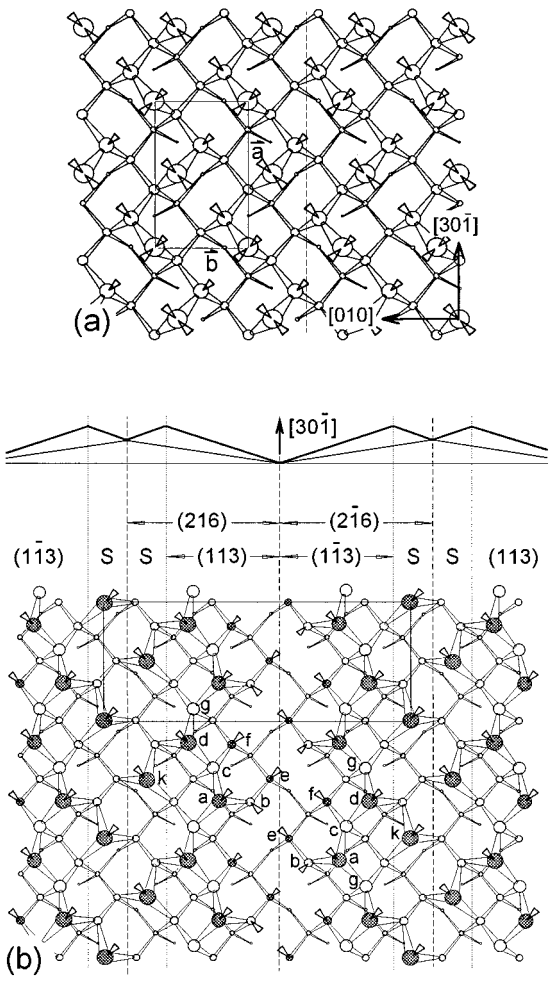

FIG. 6. (a) Schematic drawing of the truncated Ge(103) surface, with the triangles representing the dangling bonds. Also shown are a unit cell, the unit vectors a and b, and the glide line (the vertical dashed line). (b) Model of the atomic structure of the Ge(103)1×4 surface, with a 1×4 unit cell ($8.95\,\text{Å}\times22.64\,\text{Å}$) outlined. Shown on top is the side view of the surface morphology. The dashed lines are glide lines of the surface and separate the surface into (216) and (216) strips. Note that a (216) strip of this model is the same as a ''$(113)+s$'' strip of the (216) surface in Fig. 7. Note also that in this figure as well as in Figs. 7 and 8 the atoms that carry a same lower-case character are equivalents.

unit cell, thus making the surface unstable; the unit vector lengths are $a=5.66$ Å and $b=8.95$ Å. These are reflected in the atomic image: there is a glide line at the center of each ridge and valley; the surface is 1×4 reconstructed in order to reduce the number of dangling bonds; the separation between two neighboring ridges is $4b=22.64$ Å. Since each ridge consists of a (216) strip at left and a (216) strip at right, we look next at the truncated (216) surface schematically shown in Fig. 7. Obviously, the surface can be viewed as a stepped (113) surface. Luckily, the atomic structure of the (113) surface has been determined very recently [see the model in Fig. 8(b)].[40] The model shows that its surface atoms form rows lying along the [30$\bar{1}$] direction. Probably not accidentally, the width of the (113) strips that consists of the (216) surface is exactly the same as that of these (113) rows. This fact makes it quite natural to speculate that the narrow

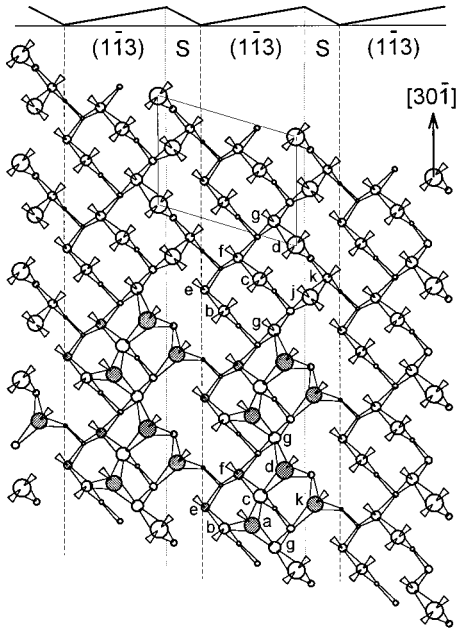

FIG. 7. Schematic drawing of the truncated (2$\bar{1}$6) surface of Ge, along with the side view of its morphology (top). Note that the lower-central portion is 1×1 reconstructed. A 1×1 unit cell of the surface is outlined. Note that the (113) strips are the same as the strip in Fig. 8(a) confined by the two dashed lines.

(11$\bar{3}$) terraces of the (2$\bar{1}$6) surface are reconstructed similarly to the (113) surface, as well as to further speculate the surface structure of the entire (216) surface as shown in the lower-central part of Fig. 7. If this speculation is correct then the atomic structure of the $(103)1\times4$ surface must be like the model shown in Fig. 6(b). To believe this model, one only needs to compare a unit cell of this model with that of the atomic image of this surface given in Fig. 5(d). Almost all surface atoms that carry a dangling bond are visible in the image at approximately right positions, except the only one that is not shaded, whose dangling bond is essentially horizontal and thus was not imaged as a protrusion in the image.

In addition to the nice agreement between the model and the atomic image, this Ge(103)1×4 model is supported by the following facts. (i) The major portion of the model surface has the $(113)3\times1$ structure that has been shown to be the structure of the Ge(113) surface,[40] which has a very low specific surface-free energy,[33,34] and shares the driving forces of reconstruction with the Ge(113) surface.[40] (ii) The model surface contains steps whose density of dangling bonds (DB) is very low, thus making the density of dangling bonds of the entire surface only $0.059\,\text{DB/Å}^2$, even lower than $0.063\,\text{DB/Å}^2$ of the Ge(001)2×1 and Ge(113) surfaces. (iii) The model surface, different from the Ge(113)3×1 surface structure, has an even number of dangling bonds, thus making the surface autocompensated so that the energy of the surface can be lowered further by opening up a gap between the highest-occupied and lowest-unoccupied surface states.[1] (iv) The model surface must have very low local strains, at least comparable to that of the Ge(113) surface, because the surface consists of *complete* rows lying along the [301] direction, of which the Ge(113) surface consists.[40] In the case of Ge(113) surface, such rows extend to thousands

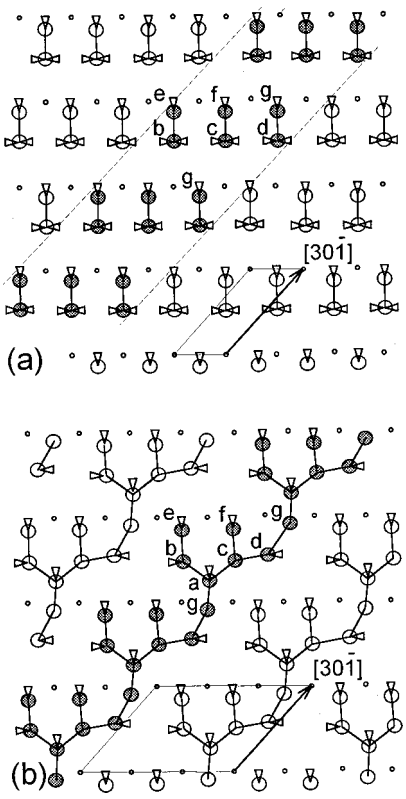

FIG. 8. (a) Schematic drawing of the truncated Ge(1$\bar{1}$3) surface, with a 1×1 unit cell outlined. If we let atom *d* form a dimer with atom *c* and then put an adatom *a* onto atoms *b*, *c*, and *g* then this surface reconstructs to the structure in (b). (b) Model of the atomic structure of the Ge(113)3×1 surface (Ref. 40). Note that the topmost atoms of the surface form rows parallel to the [301] direction, and atoms belonging to the row running from lower-left to upper-right are shaded for clarity. A 3×1 unit cell is outlined.

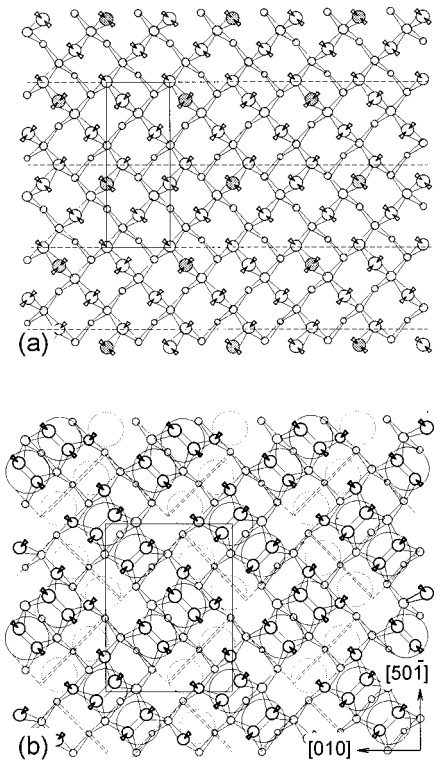

FIG. 9. (a) Schematic drawing of the truncated Ge(105) surface, with a 1×1 unit cell outlined and the triangles representing the dangling bonds. The surface consists of narrow terraces separated by steps along the dashed lines. The shaded atoms are those no longer existing in the 1×2 reconstruction. (b) Model of the Ge(105)1×2 surface, with a 1×2 unit cell outlined. The single and double-dashed lines represent the *A*-type (or SA) and *B*-type (or SB) steps (Ref. 3), respectively. The large solid and dotted circles represent the features expected to be visible in STM images of the surface.

of Å in the $3\times$ direction without a break, apparently because of its low strains.[40] Obviously, the (216) model also exhibits all these features and hence must also be physically reasonable.

Herring pointed out a long time ago that if a given macroscopic surface of a crystal does not coincide in orientation with some portion of the boundary of the equilibrium shape, there will always exist a hill-and-valley structure which has a lower free energy than the flat surface;[32] in other words, the surface will facet. Since for Si, and very likely also for Ge, {113} is a portion of the boundary of the equilibrium shape[33,34] while {103} is not, it seems to be very natural that the latter facets to the former. However, this actually is quite surprising because, on the one hand, the width of the {113} facets on the (103) surface is only about 10 Å, while, on the other hand, Herring's conclusion, is based on a phenomenological rather than atomistic approach and thus should not be expected to be able to predict any faceting where facets with atomic scales would be involved.[32] Of course, such faceting does not contradict Herring's conclusion at all, as long as the involved minifacets, such as those of the Ge(103)1×4 surface, could be sewn together without invoking high-energy edges. In the case of Ge(103)1×4 and Ge(216)1×1 surfaces, the mini {113} facet strips can indeed be connected to one another, as mentioned above, either directly or through the steps so that Herring's prediction gets realized and results in extremely narrow facet strips. Actually, a unit cell of the Si(5 5 12)2×1 surface has also been suggested to consist of minifacets of (337) and (225), very recently.[30] A natural and interesting remaining question then is why a unit cell of the (103) surface tends to consist of ''one strip of (216)+ one strip of (216)'' rather than ''*n* strips of (216)+*n* strips of (216),'' as we would expect because in the latter case the surface would have a lower density of the connecting edges. We suppose that this is so not only because the edges are of low energy but also because the small saw tooth structure of the former case, compared with the large sawtooth structure, induces less strain energy thus being more favorable.

Now, we try to find out the atomic structure of the (105) facets. Since a brief model has been proposed for (105) facets of Ge clusters grown on Si(001) (Ref. 55) we test this model first and a complete model including all details is then given in Fig. 9(b). The model is very simple: starting from the truncated (105) surface with the shaded atoms removed [Fig. 9(a)], let all terraces reconstruct into dimer rows (though only two dimers long) just like in the case of a flat Ge(001) surface; meanwhile let the straight mixed-type steps decompose into zigzag steps consisting of short segments of *A*-type and *B*-type steps.[3] To test this model with STM, as usual, we acquired pairs of filled- and empty-state images

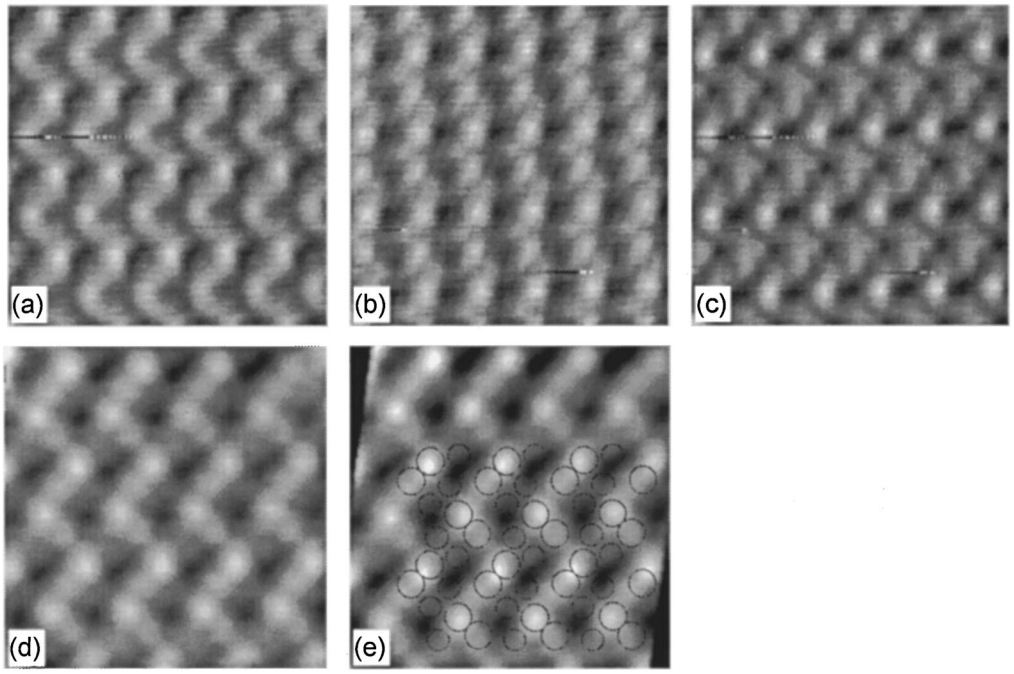

FIG. 10. STM images acquired from a Ge(105) facet on the Ge(103) surface. (a) Filled-state image, $62\,\text{Å}\times 62\,\text{Å}^2$, -1.5 V, 0.5 nA. (b) Empty-state image, $62\times 62\,\text{Å}^2$, 1.5 V, 0.5 nA, acquired simultaneously with (a). (c) Atomic image (see text) obtained from (a) and (b), $62\times 62\,\text{Å}^2$. (d) Another filled-state image but with a higher resolution than (a), $46\times 46\,\text{Å}^2$, -1.5 V, 0.5 nA. Note that the atomic image in (c) is actually very similar to this image as well as (a). (e) A portion of (d) with the major features of the Ge(105)1×2 model superimposed on. The superimposed circles correspond to the solid and dotted large circles in Fig. 9(b).

from the surface of such a facet and then obtained the atomic images from them, as shown in Fig. 10. The resolution of these images is not much better than that of the images given in Ref. 55, while getting dual bias images with a higher resolution is not easy because the back and forth switching of the polarity of the bias voltage often results in tip instability, especially for sharp tips; thus a filled-state image with better resolution is also shown in Fig. 10. As one can see, the filled-state image is very similar to the atomic image. Actually, this is quite normal and has been pointed out in many previous papers.[53,56,57] To facilitate comparison of the model with the images, in Fig. 10(e) the major features of the model are superimposed on part of the filled-state image. The dimers are at the right positions and are clearly visible in the image. Those atoms that have a dangling bond are only vaguely visible, partly because they are at lower positions and partly because their dangling bond is nearly empty as indicated by the fact that they are imaged in the empty-state images as the brightest features. Their dangling-bond charge is, very likely, transferred to the dimer that is directly connected to them, thus making that dimer brighter in the filled-state images than the other one in the same terrace.

We note that the model surface has a dangling-bond density of 0.073 DB/Å^2, which is about 16% higher than that of the Ge(001)2×1 surface, and has half of its total step length as *B*-type, which has a much higher energy than *A*-type steps.[3] These seem to be the weakness of the model. However, a recent *ab initio* molecular-dynamics study shows that the energy of nonrebonded (especially buckled nonrebonded) *B*-type steps can be much lower than that of rebonded ones,[13] while what Chadi calculated is just rebonded ones[3] and what appears in the model is just nonrebonded (very possibly buckled nonrebonded) ones. Therefore, containing *B*-type steps does not necessarily mean that the model is unfavorable. Moreover, that seems to be a very important driving force behind the reconstruction of the Ge(105) surface, because it makes the surface like a checkerboard, which might be the ideal mosaic pattern of the stress domains for surfaces like this to reduce their strain energy.[5] This, of course, needs to be tested in future investigations, because almost only vicinal surfaces in the [100] azimuth have been carefully studied[3–10] and hence, only the particular striped mosaic pattern of the stress domains has been treated theoretically so far.[5,6,8–10] On the other hand, this is also very interesting and challenging. The question here is a quantitative rather qualitative one: could the net domain-wall energy[5] become negative when the domain size is as small as that in the Ge(105)1×2 model? In the model the domains are only about two dimers in size and the domain walls are the steps. To answer this question, atomistic calculations are necessary. In this regard, recent *ab initio* molecular-dynamics investigations have shown that there is plenty of room for stepped surfaces to reduce their energy,[13] while atomistic calculations using the Stillinger-Weber interatomic potential have shown that stress relaxation can lower the en-

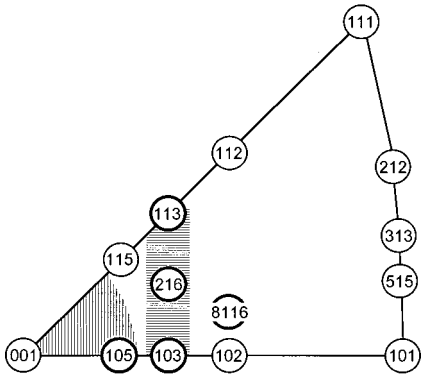

FIG. 11. Unit stereographic triangle of Ge surfaces, showing the stable surfaces determined in our works (thick circles) and in previous LEED works (Ref. 52) (thin circles). The territory of the (001) and (113) family is shaded with vertical and horizontal thin lines, respectively.

ergy of a Si(001) stepped surface below that of the flat surface.[8]

So far we have discussed the atomic structure of the Ge(103), (216), and (105) surfaces and have seen that the former two consist of only stripped (113) terraces along with steps thus belonging to the (113) family while the latter consists of only mini (001) terraces along with steps thus belonging to the (001) family. This relationship is shown in Fig. 11 with a unit stereographic triangle of Ge surfaces. Apparently, we have just started to fill the triangle up with information. As the next step, investigation of the (hhk) surfaces that have their projection lying around (113) is under way, and the preliminary results have shown that they are quite different from their Si counterpart.[42]

SUMMARY

To summarize, we have studied the clean and well-annealed Ge(103) surface with STM and LEED, and the following results have been obtained.

(i) The surface morphology consists of large 1×4 reconstructed (103) terraces along with a same kind of tentlike protrusions, which are formed with (105), {216}, and, very possibly, {8 1 16} facets.

(ii) For further investigations an atomic model has been proposed for the $(103)1\times4$, the $(216)1\times1$, and the $(105)1\times2$ reconstructions, on the basis of their high-resolution dual-bias images.

(iii) The $(103)1\times4$ surface reconstruction consists of stripped {216} terraces with a width of only one unit-vector length, while the (216) facets in turn consist of the stripped (113) terraces with a width of also only one unit-vector length.

(iv) The $(105)1\times2$ surface consists of the smallest $(001)2\times1$ terraces containing only two dimers as well as short segments of A-type and B-type steps. The terraces form a checkerboard pattern, which is expected to be typical for vicinal (001) surfaces of Si and Ge in the [100] azimuth direction, thus implying a stress-relaxation driving force behind this reconstruction.

(v) These surface structures indicate that Herring's faceting theorem can be valid down to atomic scales, provided that the atomic-scaled facets could be connected into a large surface by low-energy edges and/or corners. This fact further indicates that faceting of a surface does not necessarily mean that the surface is thermodynamically unstable, although it is generally thought to be so.[32]

ACKNOWLEDGMENTS

This work was supported by the National Natural Science Foundation of China and the Doctoral Program Foundation of the Education Ministry of China.

*Author to whom correspondence should be addressed. Electronic address: wsyang@svr.bimp.pku.edu.cn

[1] J. P. LaFemina, Surf. Sci. Rep. **16**, 133 (1992), and references therein.
[2] D. Haneman, Rep. Prog. Phys. **50**, 1045 (1987), and references therein.
[3] D. J. Chadi, Phys. Rev. Lett. **59**, 1691 (1987).
[4] F. K. Men, W. E. Packard, and M. B. Webb, Phys. Rev. Lett. **61**, 2469 (1988).
[5] O. L. Alerhand, D. Vanderbilt, R. D. Meade, and J. D. Joannopoulos, Phys. Rev. Lett. **61**, 1973 (1988).
[6] O. L. Alerhand, A. N. Berker, J. D. Joannopoulos, D. Vanderbilt, R. J. Hamers, and J. E. Demuth, Phys. Rev. Lett. **64**, 2406 (1990).
[7] B. S. Swartzentruber, Y.-W. Mo, R. Kariotis, M. G. Lagally, and M. B. Webb, Phys. Rev. Lett. **65**, 1913 (1990).
[8] T. W. Poon, S. Yip, P. S. Ho, and F. F. Abraham, Phys. Rev. Lett. **65**, 2161 (1990).
[9] E. Pehlke and J. Tersoff, Phys. Rev. Lett. **67**, 465 (1991).
[10] E. Pehlke and J. Tersoff, Phys. Rev. Lett. **67**, 1290 (1991).
[11] E. Pehlke and J. Tersoff, Phys. Rev. Lett. **68**, 816 (1992).
[12] R. M. Tromp and M. C. Reuter, Phys. Rev. Lett. **68**, 820 (1992).
[13] P. Boguslawski, Q.-M. Zhang, Z. Zhang, and J. Bernhole, Phys. Rev. Lett. **72**, 3694 (1994).
[14] A. Oshiyama, Phys. Rev. Lett. **74**, 130 (1995).
[15] X. Tong and P. A. Bennet, Phys. Rev. Lett. **67**, 101 (1991).
[16] E. Schröder-Bergen and W. Ranke, Surf. Sci. **259**, 323 (1991).
[17] J. Wasserfall and W. Ranke, Surf. Sci. **315**, 227 (1994).
[18] M. Hanbücken, B. Röttger, H. Neddermeyer, Surf. Sci. **331-333**, 1028 (1995).
[19] R. J. Phaneuf and E. D. Williams, Phys. Rev. Lett. **58**, 2563 (1987).
[20] R. J. Phaneuf, E. D. Williams, and N. C. Bartelt, Phys. Rev. B **38**, 1984 (1988).
[21] D. Y. Noh, K. I. Blum, M. J. Ramstad, and R. J. Birgeneau, Phys. Rev. B **44**, 10 969 (1991).
[22] D. Y. Noh, K. I. Blum, M. J. Ramstad, and R. J. Birgeneau, Phys. Rev. B **48**, 1612 (1991).
[23] W. Ranke, Phys. Rev. B **41**, 5243 (1990).
[24] U. Myler, P. Althainz, and K. Jacobi, Surf. Sci. **251/252**, 607 (1991).
[25] U. J. Knall, J. B. Pethica, J. D. Todd, and J. H. Wilson, Phys. Rev. Lett. **66**, 1733 (1991).
[26] D. M. Bird, L. J. Clark, R. D. King-Smith, M. C. Payne, I. Stich, and A. P. Sutton, Phys. Rev. Lett. **69**, 3785 (1992).
[27] J. Dabrowski, H.-J. Müssig, and G. Wolff, Phys. Rev. Lett. **73**, 1660 (1994).
[28] S. Song and S. G. J. Mochrie, Phys. Rev. B **51**, 10 068 (1995).
[29] A. A. Baski and L. J. Whitman, Phys. Rev. Lett. **74**, 956 (1995).
[30] A. A. Baski, S. C. Erwin, and L. J. Whitman, Science **269**, 1556 (1995).
[31] S. C. Erwin, A. A. Baski, and L. J. Whitman, Phys. Rev. Lett. **77**, 687 (1996).
[32] C. Herring, Phys. Rev. **82**, 87 (1951).
[33] D. J. Eaglesham, A. E. White, L. C. Feldman, N. Moriya, and D. C. Jacobson, Phys. Rev. Lett. **70**, 1643 (1993).
[34] J. M. Bermond, J. J. Métois, X. Egéa, and F. Floret, Surf. Sci. **330**, 48 (1995).
[35] H. Neddermeyer and St. Tosch, Phys. Rev. B **38**, 5784 (1988), and references therein.
[36] J. C. Fernandez, W. S. Yang, H. D. Shih, F. Jona, D. W. Jepsen, and P. M. Marcus, J. Phys. C **14**, L55 (1981).
[37] W. S. Yang, X.-D. Wang, K. Cho, J. Kishimoto, S. Fukatsu, T. Hashizume, and T. Sakurai, Phys. Rev. B **50**, 2406 (1994).
[38] W. S. Yang and F. Jona, Phys. Rev. B **29**, 899 (1984).
[39] Zheng Gai, Hongbin Yu, and W. S. Yang, Phys. Rev. B **53**, 13 547 (1996).

[40] Zheng Gai, Hang Ji, Bo Gao, R. G. Zhao, and W. S. Yang, Phys. Rev. B **54**, 8593 (1996).
[41] Zheng Gai, R. G. Zhao, and W. S. Yang, preceding paper, Phys. Rev. B **56**, 12 300 (1997).
[42] Zheng Gai, R. G. Zhao, Xiaowei Li, and W. S. Yang (unpublished).
[43] Yun Zhang, R. G. Zhao, and W. S. Yang, Surf. Sci. Lett. **293**, L821 (1993).
[44] R. G. Zhao, Yun Zhang, and W. S. Yang, Phys. Rev. B **48**, 8462 (1993).
[45] W. S. Yang, X.-D. Wang, K. Cho, J. Kishimoto, T. Hashizume, and T. Sakurai, Phys. Rev. B **51**, 7571 (1995).
[46] Zheng Gai, Hang Ji, Yi He, Chuan Hu, R. G. Zhao, and W. S. Yang, Surf. Sci. Lett. **338**, L851 (1995).
[47] Zheng Gai, R. G. Zhao, Yi He, Hang Ji, Chuan Hu, and W. S. Yang, Phys. Rev. B **53**, 1539 (1996).
[48] Hang Ji, R. G. Zhao, and W. S. Yang, Surf. Sci. **371**, 349 (1997).
[49] Zheng Gai, Bo Gao, Hang Ji, R. G. Zhao, and W. S. Yang, Surf. Rev. Lett. (to be published).
[50] Zheng Gai, R. G. Zhao, Bo Gao, Hang Ji, and W. S. Yang, Surf. Sci. (to be published).
[51] Hang Ji, Xiaowei Li, R. G. Zhao, Zheng Gai, and W. S. Yang, Surf. Sci. (to be published).
[52] B. Z. Olshanetsky and V. I. Mashanov, Surf. Sci. **111**, 429 (1981).
[53] J. Tersoff and D. R. Hamann, Phys. Rev. B **31**, 805 (1985).
[54] Zheng Gai, R. G. Zhao, Hang Ji, and W. S. Yang (unpublished).
[55] Y.-W. Mo, D. E. Savage, B. S. Swartzentruber, and M. G. Lagally, Phys. Rev. Lett. **65**, 1020 (1990).
[56] M. Tsukada, S. Watanabe, and T. Schimizu, in *The Structure of Surfaces IV*, edited by Xide Xie *et al.* (World Scientific, Singapore, 1994), p. 39.
[57] W. S. Yang, X.-D. Wang, K. Cho, J. Kishimoto, T. Hashizume, and T. Sakurai, Phys. Rev. B **51**, 7571 (1995).